SERI/PR-9330-1-T3
(DE82000228)
Distribution Category UC-63

Progress Report No. 3

PREPARATION AND PROPERTIES OF EVAPORATED CdTe FILMS COMPARED WITH SINGLE CRYSTAL CdTe

May 1 - July 31, 1981

Subcontract No. XW-1-9330-1

Solar Energy Research Institute
Department of Energy
Golden, Colorado

Richard H. Bube, Principal Investigator

Alan L. Fahrenbruch, Senior Research Associate
Walter Huber, Post-Doctoral Fellow
Charles Fortmann and Thomas Thorpe, Graduate Research Assistants

Department of Materials Science and Engineering
Stanford University
Stanford, California 94305

ABSTRACT

Preparation of the hot-wall vacuum deposition system nears completion and the first trial evaporation should take place in mid October. A UTI 100C Mass Analyser with a 1 to 300 AMU capability has been ordered for the system. Preliminary tests indicate good temperature tracking between the furnace core and the CdTe source itself.

Homojunction cells prepared by HWVE deposition of n-CdTe on p-CdTe substrates in October 1980 show no significant change in dark or light properties after open-circuit storage for the next 9 months.

CdTe single crystal boules have been grown with P, As and Cs impurity. For P impurity it appears from our data that the segregation coefficient is close to unity, that the value of hole density is controlled by the P and not by some unknown background acceptor, and that growth with excess Cd gives slightly higher values of hole density than growth with excess Te. CdTe:As crystals appear similar to CdTe:P crystals.

Grain boundary resistivity has been measured for single grain boundaries in two p-type CdTe:As samples, two p-type CdTe:P samples, and two n-type CdTe:In samples. Grain boundary resistivities in the 1-10 ohm-cm p-type samples have values lying between about 10^3 and 10^4 ohm-cm^2; in the 0.2-0.5 ohm-cm n-type samples the values are lower at 0.5 and 48 ohm-cm^2. Thermal activation energies of the grain boundary dark resistivity fall between 0.25 and 0.65 eV. Illumination decreases the resistivity and the activation energy, while increasing the capacitance of these grain boundaries. Wavelengths near the bandgap of CdTe are most effective. Light appears to decrease the grain boundary resistivity only below 180^{o}C; above that temperature the photoeffect disappears and a single curve is measured in dark and under illumination. A possible model is that low-temperature transport is by photo-modulated tunneling, while higher-temperature transport is by excitation over the barrier.

EVAPORATED CdTe FILMS

Hot-Wall Vacuum Deposition System

The Varian 3118 diffusion pump system has been installed and tested, indicating a pressure in the low 10^{-8} Torr range. Except for a few remaining small parts, all the fixturing and feedthroughs have been received and are assembled. The first complete retort has also been assembled. The heater power supplies, including four separate Eurotherm Model 919 temperature controllers with variacs for load matching, have been completed and tested. Complete assembly of the system (with the residual gas analyzer discussed below) and mechanical trials are expected to be accomplished by October 6, 1981. The system will then be taken apart and cleaned for high vacuum. The first trial evaporation should take place in mid October.

Additional funds from SERI to upgrade the residual gas analysis capabilities of the deposition system were requested and granted. In the original contract we had requested a less sensitive Residual Gas Analyzer (RGA) with a limited mass range in order to identify gases in the deposition chamber that would affect growth and properties of the polycrystalline layers. This is especially important since oxygen is known to affect grain boundaries strongly in II-VI compound materials; an estimate of tolerable (or perhaps beneficial) residual gas concentration during growth is required to evaluate the possibilities of commercial scale-up. The partial pressures to be evaluated are O_2, CO, H_2O, H_2, and possibly hydrocarbon fractions from outgassing and the diffusion pump.

It has become clear that by increasing the mass number capability of the RGA to 300 AMU, a new field of information about the incorporation of dopant species into the growing layer becomes available. The most likely dopants to be used for the p-type layers are P, As, and perhaps Bi. On evaporation most of the phosphorus goes off as P_4 (M = 124), arsenic

as As_4 (M = 300), and Bi as Bi (M=209). From the work of Smith at Perkin-Elmer, it appears that it may be required to split the large molecules (into P or P_2, for example) in order to incorporate them (this might be accomplished with a high temperature zone or by RF discharge.

We have ordered a UTI 100C Mass Analyser with a 1 to 300 AMU capability that will enable us to evaluate the flux of dopant at the substrate level, by putting a pin-hole there and monitoring the flux above with the RGA as shown in Figure 1. Rotation of the entire bell jar/RGA assembly will enable the RGA to be placed above either of the two hot-wall vacuum evaporator retorts or above a resistance evaporation work station also built into the system. The RGA is usable up to 10^{-5} Torr and the minimum detectable partial pressure is 10^{-14} Torr. It is mounted in an adaptor housing with an in-line valve to reduce exposure to contamination when not in use and to permit the future addition of a small appendage pump to facilitate obtaining "zero" reference scans. The valve arrangement will also enable the future shared use of the instrument on a system with a much smaller volume to monitor desorption of gases from the grain boundaries of polycrystalline layers upon heating.

Thermal Analysis

Since the thermocouple monitoring temperature in various parts of the quartz hot-wall vacuum evaporator liner tube must be mounted outside of the tube, the thermal coupling between the stainless steel furnace cores and the evaporant charges was investigated. (To insure good temperature regulation, the controller thermocouples must be conductively coupled to the furnace core on which the heating element is wound. Auxiliary thermocouples might be radiatively coupled to the quartz liner, but to mount them in conductive contact with the CdTe would either complicate fabrication - if mounted in a re-entrant quartz

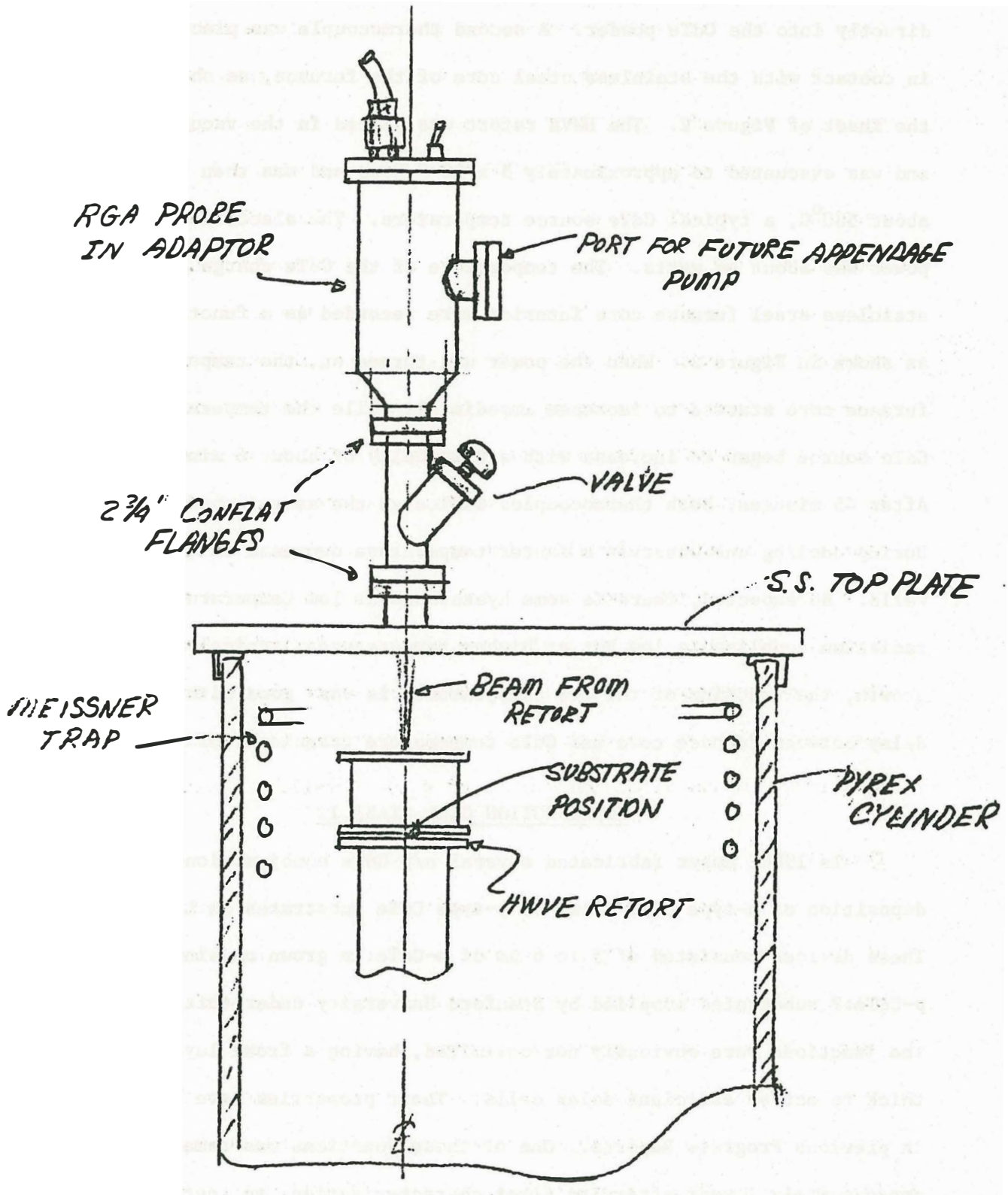

Figure 1. Configuration of the Residual Gas Analyzer above the hot-wall retort.

sheath, or risk contamination - if mounted in actual contact with the CdTe.) A quartz tube was loaded with CdTe powder and a thermocouple was inserted directly into the CdTe powder. A second thermocouple was placed inside and in contact with the stainless steel core of the furnace, as shown in the inset of Figure 2. The HWVE retort was placed in the vacuum chamber and was evacuated to approximately 5×10^{-8} Torr and was then heated to about $580^{\circ}C$, a typical CdTe source temperature. The electrical input power was about 46 watts. The temperature of the CdTe charge and of the stainless steel furnace core interior were recorded as a function of time as shown in Figure 2. When the power was turned on, the temperature of the furnace core started to increase immediately while the temperature of the CdTe source began to increase with a time delay of about 6 minutes. After 45 minutes, both thermocouples indicated the same temperature. During cooling one observes a faster temperature decrease of the furnace walls. As expected, there is some hysteresis at low temperatures when radiation coupling is low, but at higher temperatures, typical of film growth, the tracking of the two temperatures is very good with a time delay between furnace core and CdTe temperature transients of 1 to 2 minutes.

HOMOJUNCTION CELL STABILITY

In 1980, Huber fabricated several n/p CdTe homojunctions by HWVE deposition of n-type CdTe films on p-type CdTe substrates in Linz, Austria. These devices consisted of 5 to 6 μm of n-CdTe:In grown on single crystal p-CdTe:P substrates supplied by Stanford University under this contract. The junctions were obviously not optimized, having a front layer much too thick to act as efficient solar cells. Their properties have been reported in previous Progress Reports. One of these junctions was remeasured, approximately 1 year after its first characterization, to test stability. Storage was in room air and light, at open circuit. The measurements are summarized here (for simulated AM1.5 radiation).

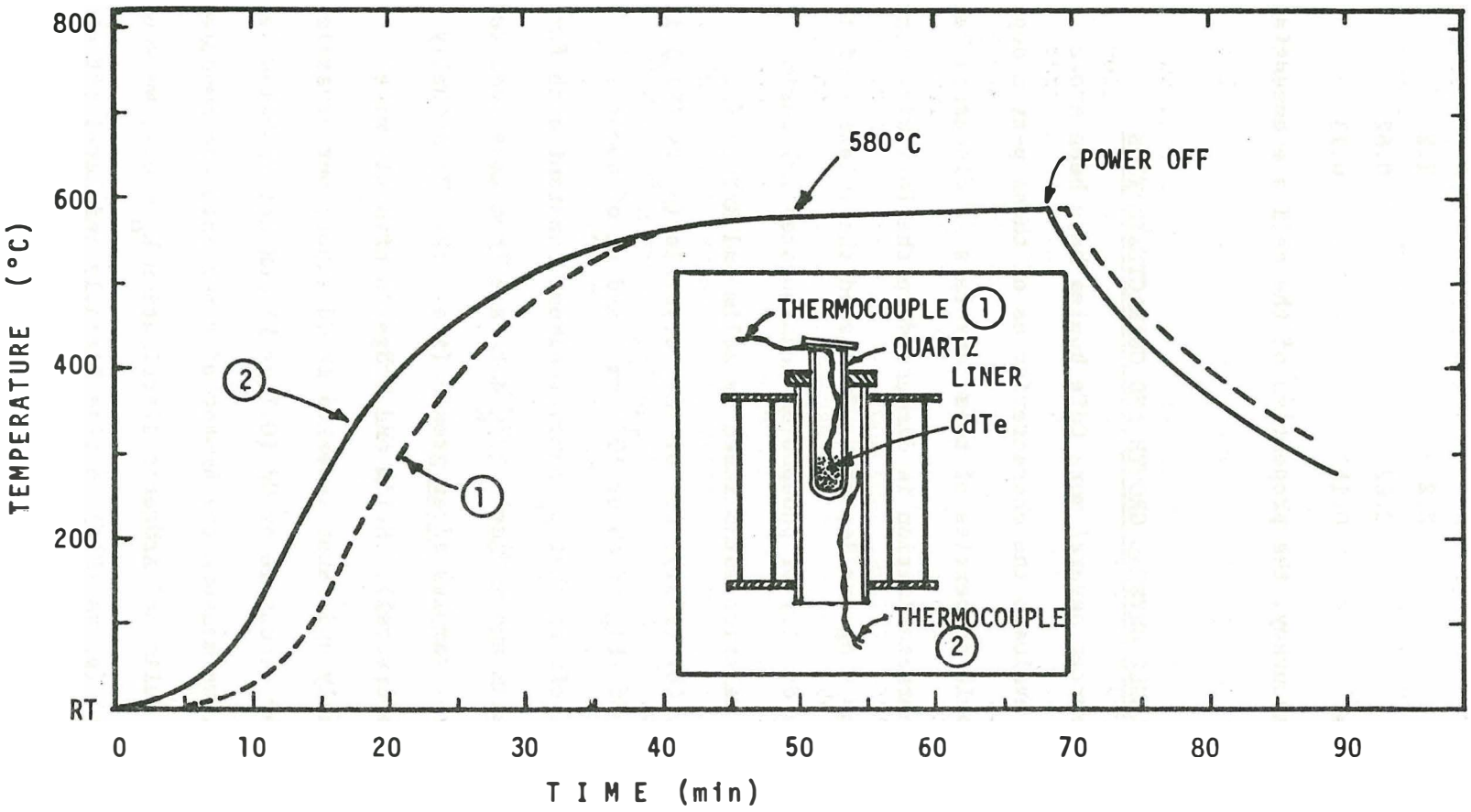

Fig. 2. The temperature of the CdTe charge (1) and of the furnace interior (2) as a function of the time. A CdTe film was deposited on the quartz cover of the retort liner during the test.

	October 1980	July 1981
J_o, A/cm^2	3 x 10^{-10}	4 x 10^{-10}
A factor	2.2	2.2
V_{oc}, V	0.62	0.62
J_{sc}, mA/cm^2	0.15	0.13

Within experimental accuracy, the properties of the cell are essentially unchanged.

SINGLE CRYSTAL GROWTH AND CHARACTERIZATION

In the past quarter several more CdTe boules have been grown with P, As and Cs to evaluate the characteristics of these p-type dopants. Measurements of the bulk properties of these crystals is discussed here and grain boundary characterization is discussed in the following section.

In the previous Progress Report we discussed the relation of the hole density p to the density of phosphorus incorporated (P) during crystal growth. The relation established by Selim and Krüger (J. Electrochem.Soc. 124, 401 (1977)) for similar crystals (p_K vs $(P)_K$) is linear up to a value of $(P)_K$ of about 10^{17} cm^{-3} and p_K of about 10^{17} cm^{-3}, after which it levels off so that p_K remains almost constant with further increase in $(P)_K$. Selim and Krüger's $(P)_K$ data are from mass spectroscopic analysis of the crystal samples after growth (i.e., the (P) actually incorporated into the crystal). Selim and Krüger's crystals were grown stoichiometrically and later annealed in Cd vapor; our crystals were grown with either excess Te or Cd (0.1 at.%) and not annealed later. For our CdTe growths, we measure the amount of P put into the ampoule before growth. Thus, given Selim and Krüger's distribution $k_o = 0.1$, we would have expected our data (p_S vs $(P)_S$) to rise linearly and level off at $p_S = 10^{17}$ cm^{-3} and $(P)_S = 10^{18}$ cm^{-3}. In fact, reduction of $(P)_S$ to 10^{17} cm^{-3} caused no significant reduction of p_S. A series of P-doped boules with lower $(P)_S$ have been grown to investigate this effect, a necessary step in establishing

a connection between dopant input and resulting carrier density. The last P growth have been with $(P)_S = 10^{15}$ and 10^{16} cm^{-3}, with either excess Cd or Te to establish the boundary of the plateua. Our preliminary data suggest that:

(1) For our growth conditions $k_o = 1$, rather than 0.1.

(2) The value of p does in fact decrease with decreasing (P) for (P) less than 10^{17} cm^{-3}. Early on we had been concerned that another unknown p-type dopant was dominating the effect of the P, causing p to be almost independent of (P). These concerns are not supported by these data.

(3) The growth with excess Cd appears to give slightly higher values of p than the previous growths with excess Te.

The P-series growths have been essentially completed, although more electrical measurements need to be done to make the conclusions more certain.

Measurements of the first As-doped boule (grown with excess Te) show a resistivity of 2 to 10 ohm-cm, with carrier densities and a p/(As) ratio similar to those found for CdTe:P. The second As boule (excess Cd) and the Cs boule (excess Cd) have been grown but not analyzed. A summary of the boules grown and to be grown in the near future is given in Table I.

TABLE I

Summary of CdTe Crystal Growths[a]

No.	Regrown	Dopant	N_A introduced, cm^{-3}	Excess[b]	Start ρ, ohm-cm	Start p, cm^{-3}	Start μ, $cm^2/V\text{-}sec$	Middle p, cm^{-3}
1	No	P	$8x10^{15}$	Te	630	$6x10^{13}$	165	$2x10^{14}$
2[c]	No	P	$8x10^{16}$	Te	130	$1x10^{16}$	40	$4x10^{16}$
3	Yes	P	$8x10^{16}$	Cd	2.4	$1x10^{16}$	120	$2x10^{17}$
4	Yes	P	$8x10^{14}$	Cd	4-20			
5	Yes	As	$4x10^{18}$	Te	20			
6	Yes	As	$2x10^{18}$	Cd				
7	Yes	Cs	$5x10^{17}$	Cd				
8	Yes	P	$8x10^{15}$	Cd				
9	Yes	P	$8x10^{15}$	Te				
10	Yes	Sb	(10^{18})[d]	Cd				
11	Yes	In	(10^{17})[d]	Cd				
12	Yes	As	(10^{17})[d]	(Cd)[d]				

[a] Boules 1 through 8 had been grown up to October 1, 1981.

[b] Calculated from input to growth ampoule after regrowth.

[c] At least 6 boules of this particular P density and excess Te have been grown on other projects.

[d] Boules 13 to 18 are not yet determined; depend on properties of previous boules.

PROPERTIES OF GRAIN BOUNDARIES

In the past quarter six grain boundaries, contained in samples cut from three CdTe boules, have been investigated. Two of the six came from an n-type CdTe:In boule with measured bulk resistivity of between 0.2 and 0.5 ohm-cm. The remaining four samples were cut from p-type CdTe boules, two from a CdTe:As boule with bulk resistivity between 2 and 10 ohm-cm, and two from a CdTe:P boule with similar resistivity. As in earlier work samples were cut in rectangular shapes (2 x 2 x 8 mm^3) with a single grain boundary extending across the 2 x 2 mm^2 cross section. Contacts were evaporated on the surface perpendicular to the boundary. The measured grain boundary resistivity and the thermal activation energy for the dark conductivity for each grain boundary are given in Table II.

Four-point grain boundary resistivity values are calculated from the voltage drop on the inner pair of contacts. Bulk resistance contributions are subtracted and the resistance value is multiplied by the grain boundary area. Values range from 0.5 ohm-cm^2 (probably a twin boundary) up to 1.4 x 10^4 ohm-cm^2. The I-V characteristic of two of the samples was non-ohmic over the range measured as shown in Figure 3, and the slope at the origin was used to calculate the resitivity, ρ_{gbo}. Activation energies for ρ_{gbo} lie between 0.25 and 0.65 eV in the dark, the two extreme values both being for n-type samples.

The grain boundary resistivity is decreased by illumination. The spectral response of this effect was measured for each sample, and a typical curve is shown in Figure 4. Although wavelengths were scanned between 0.35 and 3.2 μm, a measurable response was observed only between 0.8 and 1.2 μm close to the band gap of CdTe. The maximum response corresponded to a decrease in grain boundary resistivity by a factor of 2 to 5 in the different samples; no apparent correlation was seen between

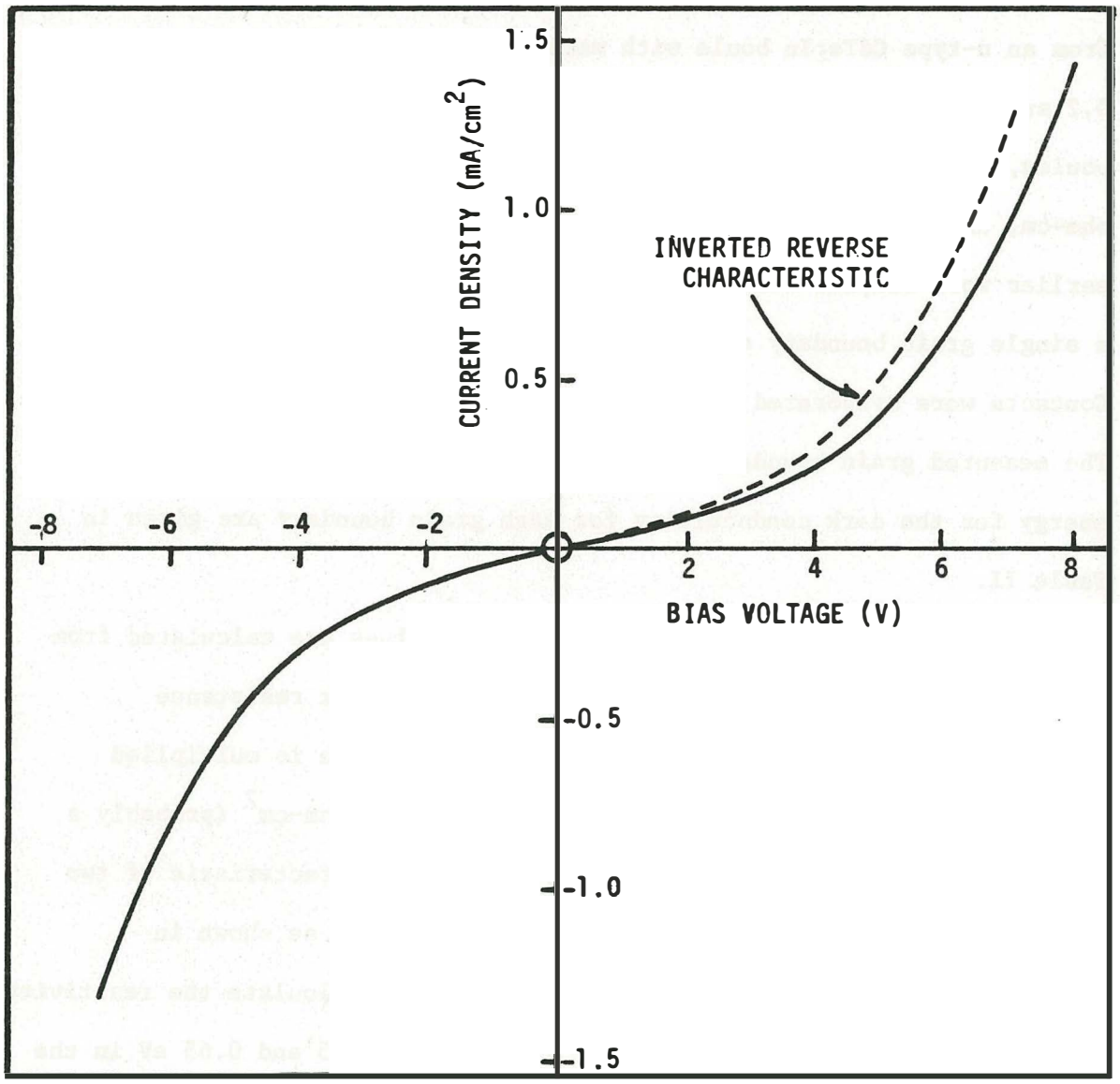

Fig. 3. J versus V characteristic of p-CdTe grain boundary. Dark, RT.

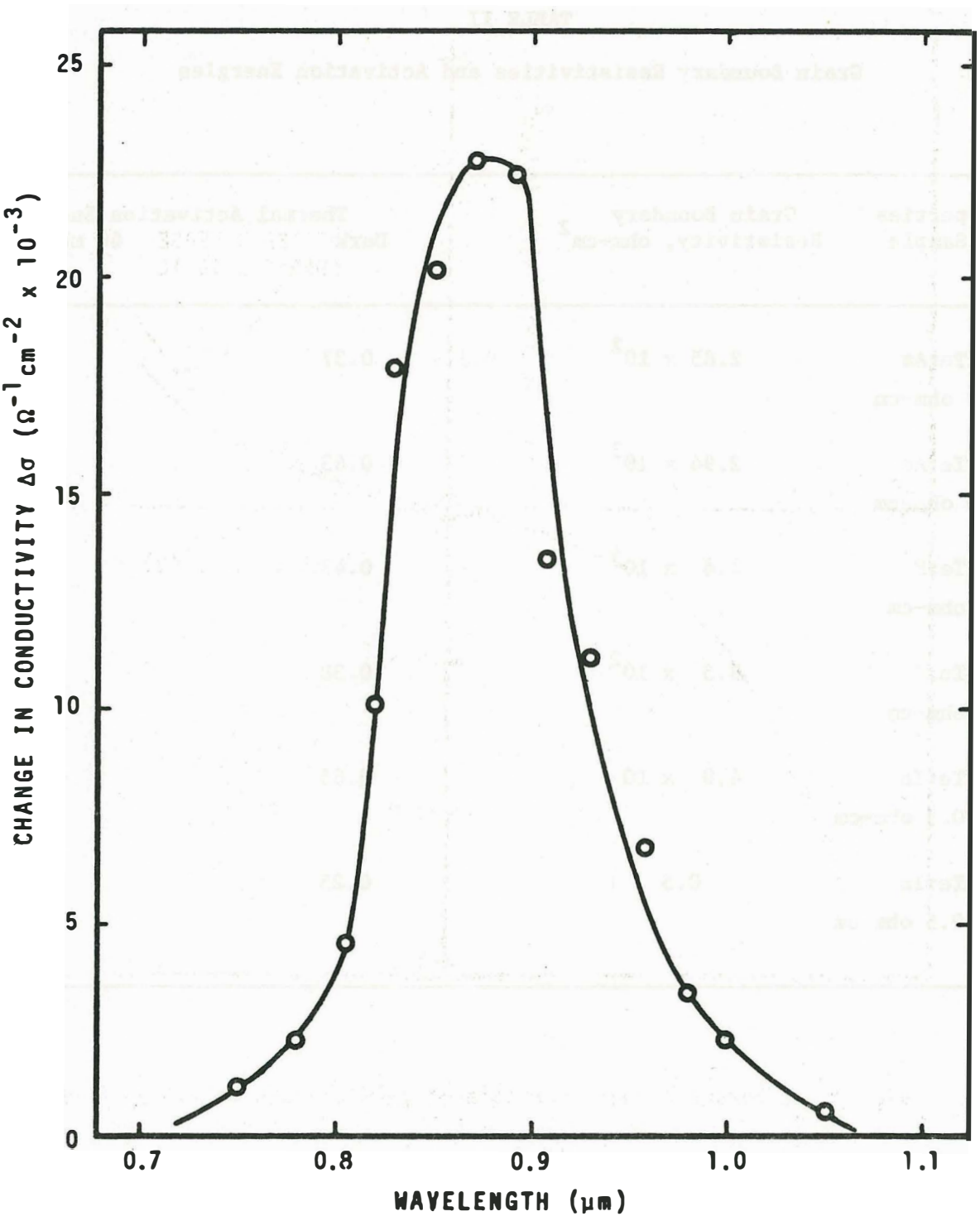

Fig. 4. Spectral response of grain boundary conductivity (RT). Dark conductivity is σ_d = 21 x 10^{-3} Ω^{-1} cm^{-2}.

TABLE II

Grain Boundary Resistivities and Activation Energies

Properties of Sample	Grain Boundary Resistivity, ohm-cm^2	Thermal Activation Energy, eV Dark	Thermal Activation Energy, eV 60 mW/cm^2 white light
p-CdTe:As 5-10 ohm-cm	2.85×10^2	0.37	0.27
p-CdTe:As 5-10 ohm-cm	2.94×10^3	0.63	0.28
p-CdTe:P 1-5 ohm-cm	1.4×10^4	0.47	0.24
p-CdTe:P 1-5 ohm-cm	8.5×10^2	0.38	0.14
n-CdTe:In 0.2-0.5 ohm-cm	4.8×10	0.65	0.48
n-CdTe:In 0.2-0.5 ohm-cm	0.5	0.25	0.19

the magnitude of the dark resistivity and the magnitude of the photoeffect.

The thermal activation energy of the grain boundary resistivity was also measured under illumination by various intensities of white light. The results are also presented in Table II. The effect of illumination is in general to decrease the activation energy. Above 180°C no photoinduced decrease in grain boundary resistivity is observed, and all curves of resistivity merge into a single curve, the same for dark and under illumination, which in general has a different activation energy from the lower-temperature light-sensitive values. Empirically the phenomenon is like that previously observed in photoconductivity in PbS films, in which the low-temperature light-sensitive region was interpreted as light-modulated tunneling through grain barriers, and the high temperature light-insensitive region was interpreted as thermal transport over the barriers.

Grain boundary capacitance was measured as a function of voltage for all six samples. The four p-type samples yielded capacitances of several hundred picofarads over the range (-2 to +2 V) measured. A $1/C^2$ vs V plot for each of these samples yielded a minimum at zero bias, as shown in Figure 5. These plots yielded carrier densities that seem to correspond relatively well to the previous bulk resistivity measurements, when the capacitance data are corrected for contact capacitance. The two n-type samples yielded capacitances of several nanofarads, and also gave reasonable carrier densities from $1/C^2$ vs V plots.

The change in capacitance induced by illumination was also measured for five of the six samples. The spectral response was quite similar to that shown for the resistivity in Figure 4. For a light intensity of about 1 mW/cm^2 the maximum values of capacitance for illumination near the bandgap of CdTe were about 1.05 to 6 times the dark capacitance.

The zero-bias capacitance was measured as a function of the

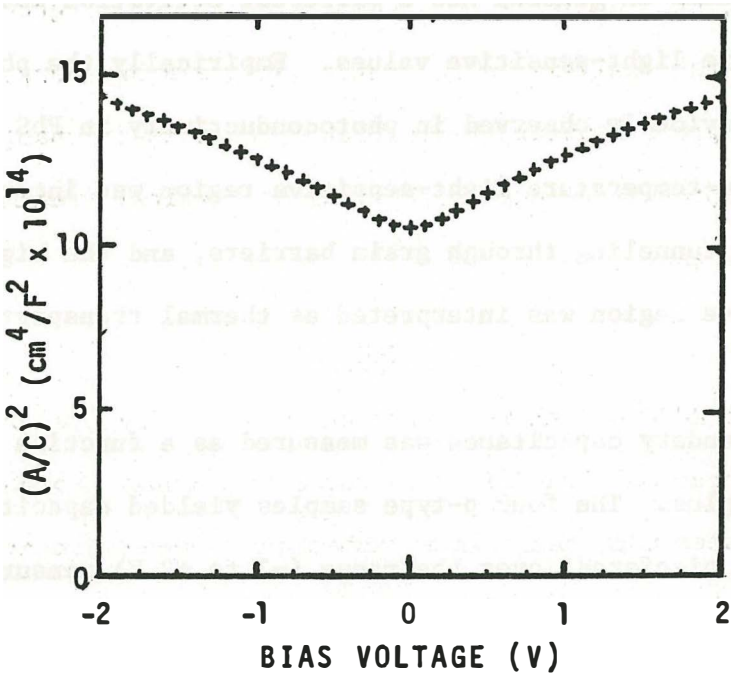

Fig. 5. Typical $1/C^2$ versus V plot for p-CdTe grain boundary (RT, dark). Uncompensated for contact capacitance.

white-light intensity. Four of the six samples showed an increase in capacitance ranging from 1.2 to 18 times the dark value (for an intensity of about 60 mW/cm^2). Two of the samples, however, actually showed a small decrease (15-20%) in capacitance when illuminated. This apparent quenching effect will be investigated further.

These samples and others suitably chosen will be further investigated using the above techniques, as well as temperature dependence of capacitance, EBIC analysis to determine diffusion lengths, atmospheric effects, and X-ray analysis to determine the grain boundary orientations. Passivation of grain boundary recombination effects or changes in grain boundary properties due to physical or chemical treatment will be investigated also.

FUTURE WORK

When the HWVE system is operational, a few initial growths will be made of undoped CdTe on BaF_2 substrates to establish a correlation between our system and that used by Huber and Lopez-Otero at Linz. It is expected that 3 to 6 films will be sufficient for this. Thickness, grain size, and optical transmission will be measured. Then a short series of n-CdTe:In films will be grown on single crystal p-CdTe:P substrates. These will serve to (1) establish a correlation to previous work at Linz, and (2) provide more samples for cell modeling studies. These studies include spectral response on cells with varying n-layer thickness that will provide minority carrier diffusion lengths (on both n- and p-type sides), surface recombination velocity, and verification of existing dependence of absorption constant on wavelength. Following this a lengthy series (both n and p) will be deposited on amorphous substrates (quartz, 7059 glass, alumina, and graphite) to determine optimum growth conditions and the variation of carrier density, mobility, and grain

boundary barrier effects on substrate temperature, dopant, and excess Te or Cd incorporation.

A table of promising cell structures is given in Table III, showing the wide variety of possibilities. We are in the process of evaluating these alternatives from the point of view of (1) probable efficiencies, (2) clarity of analytical evaluation, and (3) ease of fabrication.

TABLE III

Promising Cell Structures

No.	Substrate	Film No. 1	Film No. 2	Illumination
1	p-CdTe:P	n-CdTe:In	-	through n-CdTe:In
2	n-CdTe:In	p-CdTe:As	-	through p-CdTe:As
3	Glass/ITO	n-CdTe:In	p-CdTe:As	through glass
4	Glass/ITO	n-CdTe:In	Au	through Au
5	Glass/Au	p-CdTe:As	n-CdTe:In	either direction
6	Glass	ITO	p-CdTe:As	through glass
7	Glass	ZnO	p-CdTe:As	through glass
8	Glass	CdS	p-CdTe:As	through glass
9	Glass	SnO_x	p-CdTe:As	through glass
10	Glass[a]/metal[b]	p-CdTe:As	ITO	through ITO
11	"	p-CdTe:As	ZnO	through ZnO
12	"	p-CdTe:As	CdS	through CdS
13	"	p-CdTe:As	SnO_x	through SnO_x
14	"	n-CdTe:In	Sb_2O_3/Cr	through Sb_2O_3/Cr

[a] Glass or alumina or graphite.

[b] Metal chosen for rheotaxic and ohmic contact properties.

☆ U.S. GOVERNMENT PRINTING OFFICE: 1981-740-145/2482